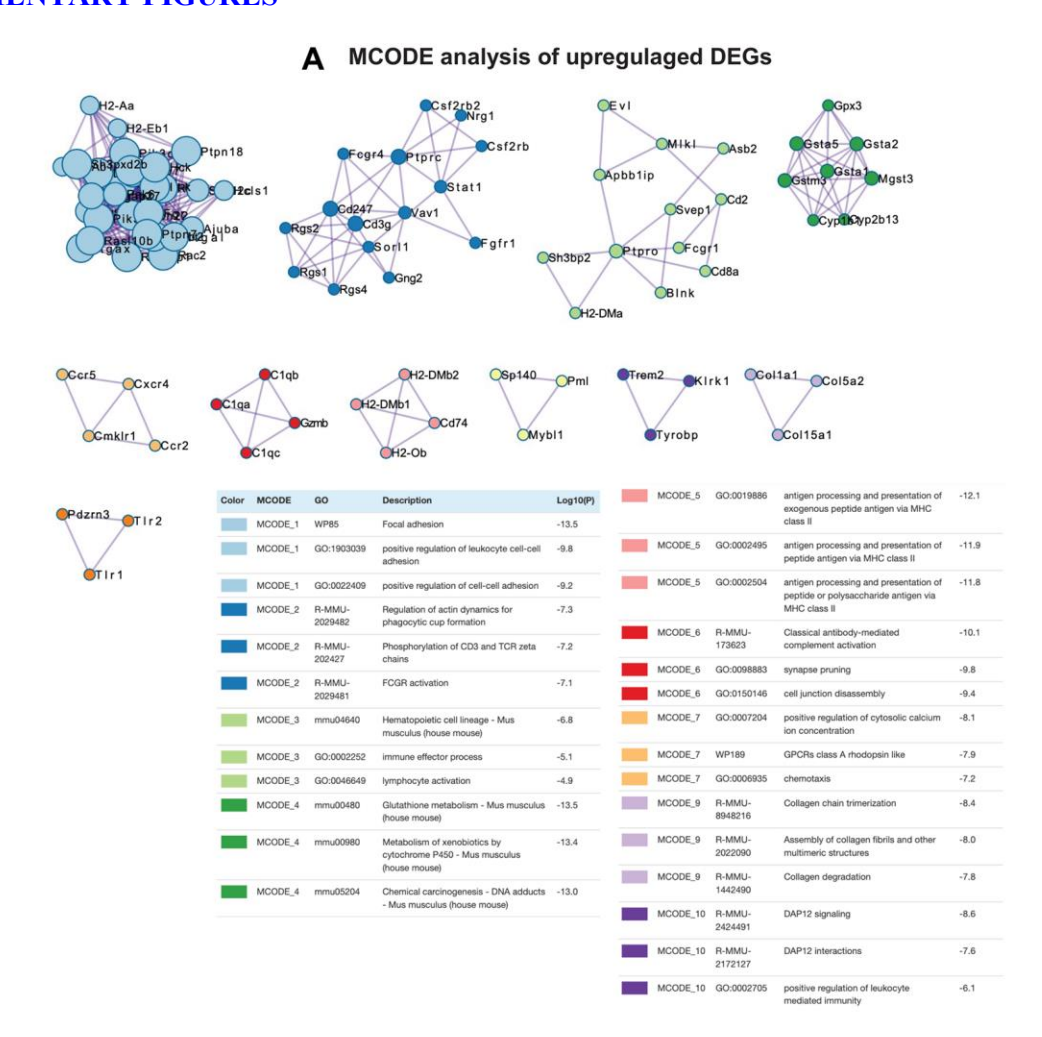
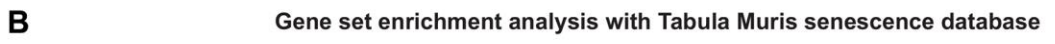
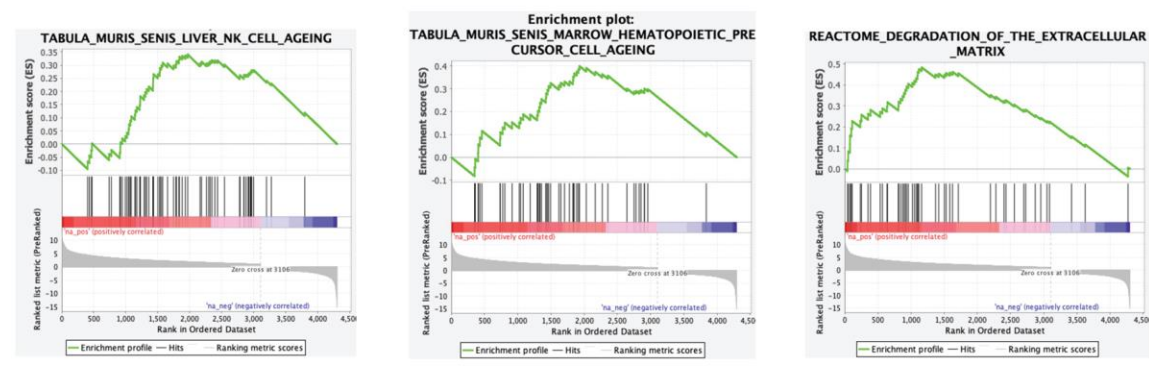
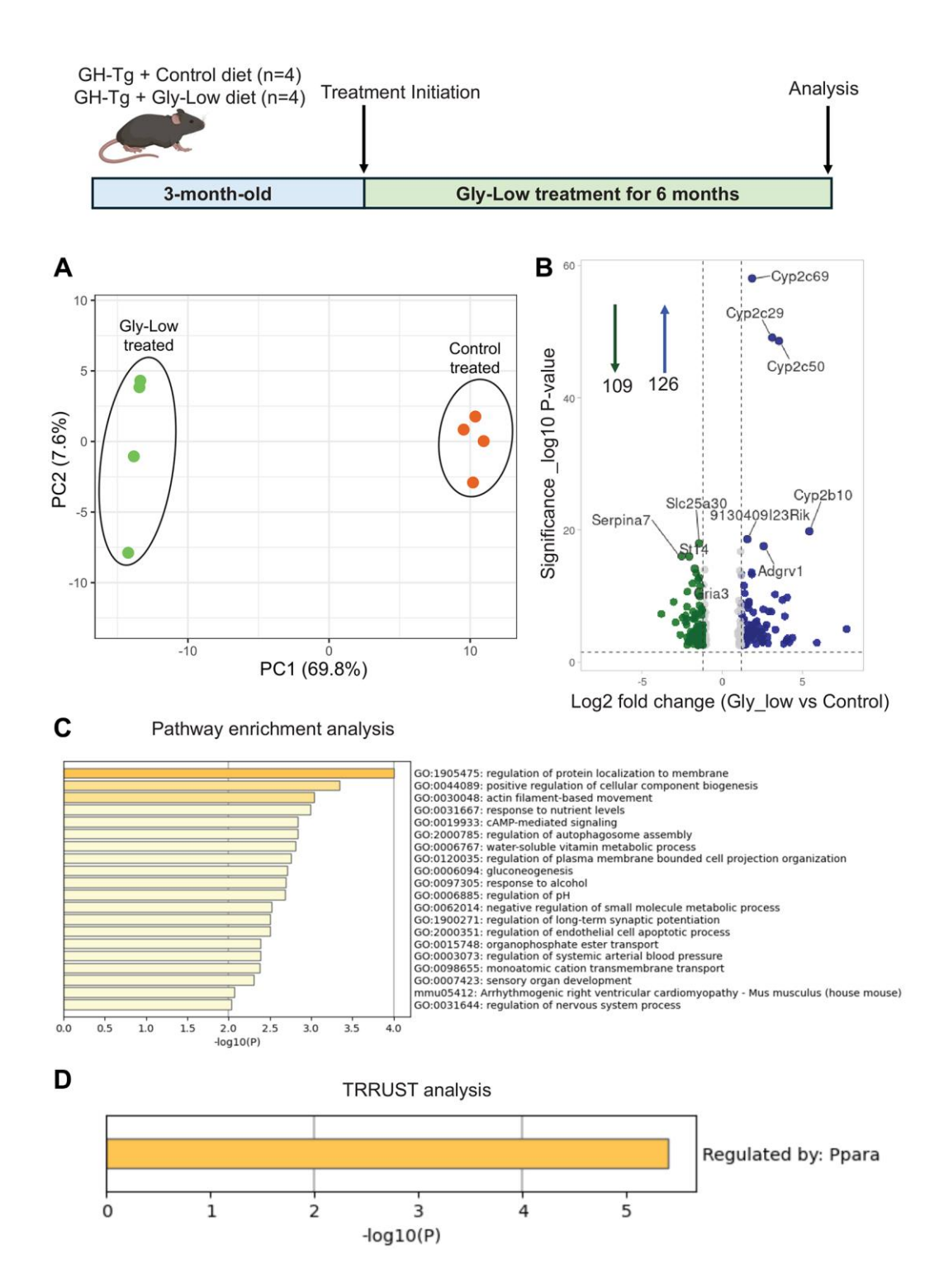
## **SUPPLEMENTARY FIGURES**



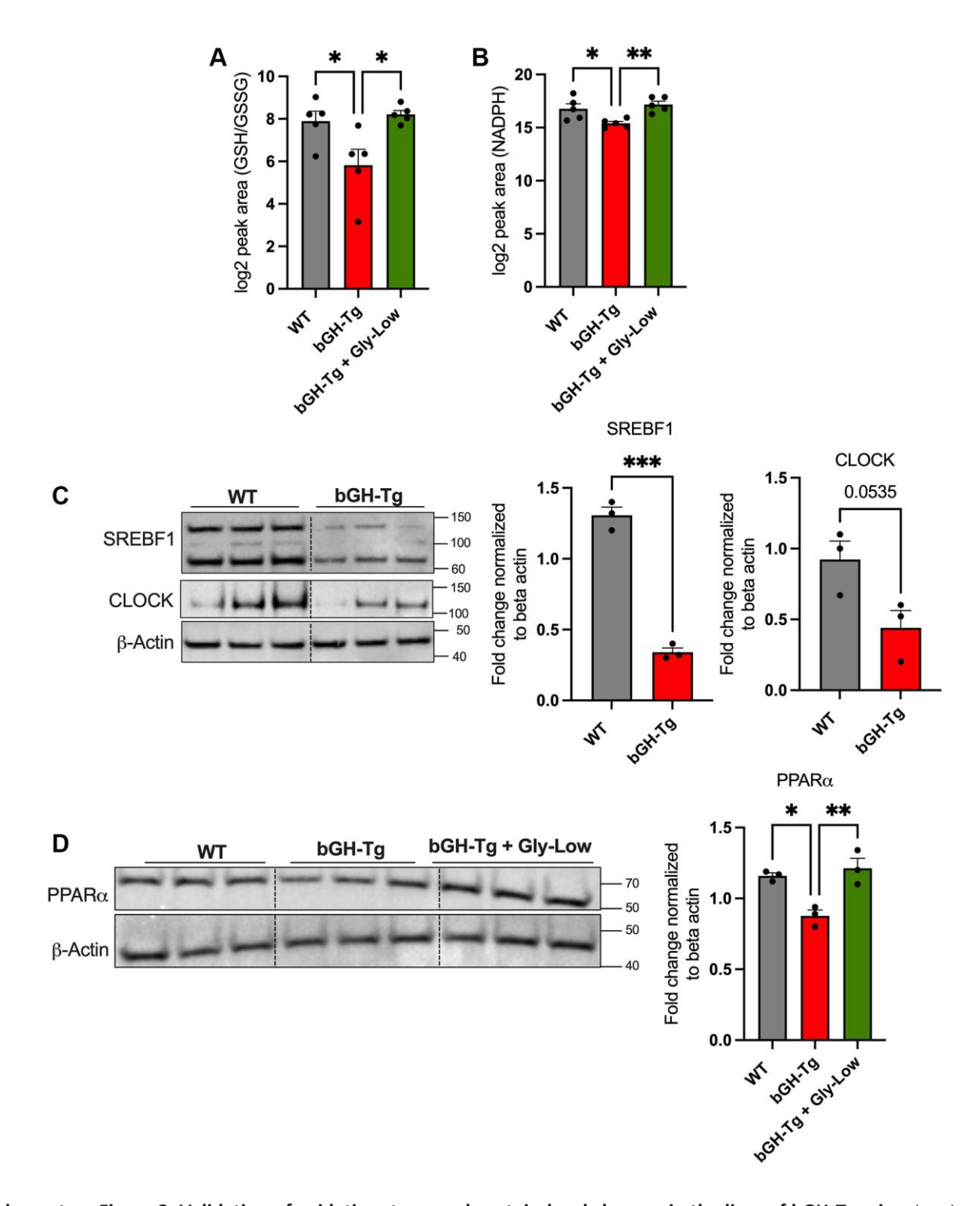




Supplementary Figure 1. Network and gene set enrichment analysis of upregulated genes in bGH-Tg liver. (A) MCODE analysis of upregulated DEGs identified protein—protein interaction network modules enriched in biological processes including focal adhesion, immune effector function, leukocyte cell—cell adhesion, regulation of antigen receptor signaling, and extracellular matrix organization, with each cluster color-coded and corresponding GO terms with enrichment scores (—log10 p) shown in the table below. (B) Gene set enrichment analysis using the Tabula Muris senescence database further highlighted significant enrichment of senescence-associated gene signatures in bGH-Tg liver, including NK cell ageing, hematopoietic precursor ageing, and extracellular matrix degradation pathways, demonstrating that GH overexpression induces transcriptional programs linked to immune activation, extracellular remodeling, and cellular senescence.



Supplementary Figure 2. Transcriptomic impact of Gly-Low treatment in the liver of bGH-Tg mice. Three-month-old WT and bGH-Tg mice were treated with either Gly-Low or control diet for 6 months, after which liver samples were collected for bulk RNA-seq analysis. Principal component analysis (A) shows distinct separation between Gly-Low-treated and control-treated bGH-Tg mice, indicating robust transcriptomic differences. Volcano plot analysis (B) identifies 235 differentially expressed genes, with 109 downregulated and 126 upregulated by Gly-Low treatment compared to control. Pathway enrichment analysis (C) reveals significant enrichment in processes including protein localization to the membrane, cellular component biogenesis, actin filament—based movement, cAMP-mediated signaling, and gluconeogenesis. TRRUST analysis (D) highlights PPARA as a key regulatory transcription factor mediating these transcriptomic changes, suggesting that Gly-Low treatment modulates metabolic and signaling pathways to mitigate GH-induced glycation stress.



Supplementary Figure 3. Validation of oxidative stress and protein-level changes in the liver of bGH-Tg mice. (A, B) Targeted metabolomic measurements of oxidative stress markers in liver tissue. GH-Tg livers show a reduced GSH/GSSG ratio (A) and decreased NADPH levels (B), indicating increased oxidative stress. Both parameters were restored by Gly-Low treatment. (C) Representative Western blots and quantification of SREBF1 (~125 kDa) and CLOCK (~100 kDa) protein levels in livers from WT and bGH-Tg mice, normalized to  $\beta$ -actin (~45 kDa). SREBF1 was significantly reduced in GH-Tg livers, while CLOCK showed a decreasing trend. (D) Western blot and quantification of PPAR $\alpha$  (~68 kDa) expression in WT, bGH-Tg, and bGH-Tg + Gly-Low livers. PPAR $\alpha$  expression was significantly decreased in GH-Tg livers and rescued by Gly-Low treatment. Data are shown as mean  $\pm$  SEM, normalized to  $\beta$ -actin for Western blots. Each dot represents an individual mouse. Significant differences are indicated:  $*p \le 0.005$ ,  $***p \le 0.0005$ .